Diffusion-trapping model of receptor trafficking in dendrites

P. C. Bressloff and B. A. Earnshaw
Department of Mathematics, University of Utah, Salt Lake City, Utah 84112, USA
(Received 13 November 2006; revised manuscript received 1 February 2007; published 26 April 2007)

We present a model for the diffusive trafficking of protein receptors along the surface of a neuron's dendrite. Distributed along the dendrite are spatially localized trapping regions that represent submicrometer mushroom-like protrusions known as dendritic spines. Within these trapping regions receptors can be internalized via endocytosis and either reinserted into the surface via exocytosis or degraded. We calculate the steady-state distribution of receptors along the dendrite assuming a constant flux of receptors inserted at one end, adjacent to the soma where receptors are synthesized, and use this to investigate the effectiveness of membrane diffusion as a transport mechanism. We also calculate the mean first passage time of a receptor to travel a certain distance along the cable and use this to derive an effective surface diffusivity.

DOI: 10.1103/PhysRevE.75.041915 PACS number(s): 87.16.Ac, 87.15.Vv

I. INTRODUCTION

The efficient delivery of proteins and other molecular products to their correct location within a cell is of fundamental importance to normal cellular function and development. Protein trafficking is of particular interest to neurobiologists due to the unique morphology and complex structure of neurons [1]. Neurons are highly polarized cells, consisting of an axon that contains ion channels for action potential propagation and protein rich presynaptic active zones for neurotransmitter release, and several dendrites containing receptors that respond to neurotransmitters. At most excitatory synapses in the brain, receptors are highly clustered at the postsynaptic density, which is the protein-rich domain in the postsynaptic membrane of a dendritic spine that is directly apposed to the presynaptic active zone. The dendritic spine is a small (submicrometer) membranous extrusion that protrudes from a dendrite. Typically spines have a bulbous head which is connected to the parent dendrite through a thin spine neck. Given that hundreds or thousands of synapses and their associated spines are distributed along the entire length of a dendrite, it follows that neurons must traffic receptors and other postsynaptic proteins over long distances (several 100 μm) from the soma or cell body (where they are synthesized) to distal regions of a dendrite. This can occur by two distinct mechanisms: either by lateral diffusion in the plasma membrane [2–4] or by motor-driven intracellular transport along microtubules followed by local insertion into the surface membrane (exocytosis) [5–7]. It is likely that both forms of transport occur in dendrites, depending on the type of receptor and the developmental stage of the organism.

In this paper we construct and analyze a model for the surface transport of AMPA (α-amino-3-hydroxy-5-methyl-4-isoxazole-propionic acid) receptors along a dendrite. These receptors respond to the neurotransmitter glutamate and mediate the majority of fast excitatory synaptic transmission in the central nervous system. [See Ref. [8] for a corresponding model of motor-driven transport, involving another class of glutamate receptor, namely, N-methyl-D-aspartate (NMDA).] We assume that surface receptors diffuse freely until they encounter a spine; if a receptor flows into a spine then it is temporarily confined by the geometry of the spine and through interactions with scaffolding proteins and cytoskeletal elements. This is consistent with single-particle tracking experiments, which show surface receptors undergoing periods of free diffusion interspersed with periods of restricted motion in confinement domains that coincide with synapses [3,9]. A surface receptor may also be internalized via endocytosis and stored within an intracellular pool, where it is either recycled to the surface via exocytosis or degraded [10]. Thus one can view the surface transport of receptors along a dendrite as a process of diffusion in the presence of spatially localized, partially absorbing traps, see Fig. 1. Studying the effects of diffusive transport within a quantitative model is important, since there is currently some experimental controversy regarding the rate of constitutive recycling via intracellular pools and the role of surface diffusion as a mechanism for delivering receptors to synapses [4,11].

In order to develop an analytically tractable model of such a process we make a number of simplifications. First, we ignore the spatial extent of each spine so that the domain over which free diffusion occurs is the whole cylindrical surface of the dendrite without excluded trapping regions. This is motivated by the observation that the spine neck, which forms the junction between a synapse and its parent dendrite, varies in radius from $\sim$0.02 to 0.2 μm [12]. This is typically an order of magnitude smaller than the spacing between synapses ($\sim$0.1–1 μm) and the circumference of the dendritic cable ($\sim$1 μm). In other words, the disklike region forming the junction between a spine and the dendritic cable (see inset of Fig. 1) is relatively small, and is therefore ignored. For simplicity, we also ignore any details of surface trafficking within a spine by treating the spine as a homogeneous domain. (For a more detailed model of receptor trafficking within a spine see Refs. [13,14].) Finally, we neglect variations in receptor concentration around the circumference of the cable relative to those along the cable by considering a reduced one-dimensional diffusion-trapping model. Under these simplifications, we obtain explicit solutions for the steady-state distribution of receptors along the dendrite and the mean first passage time for a receptor to travel a fixed distance from the soma. This allows us to determine how the

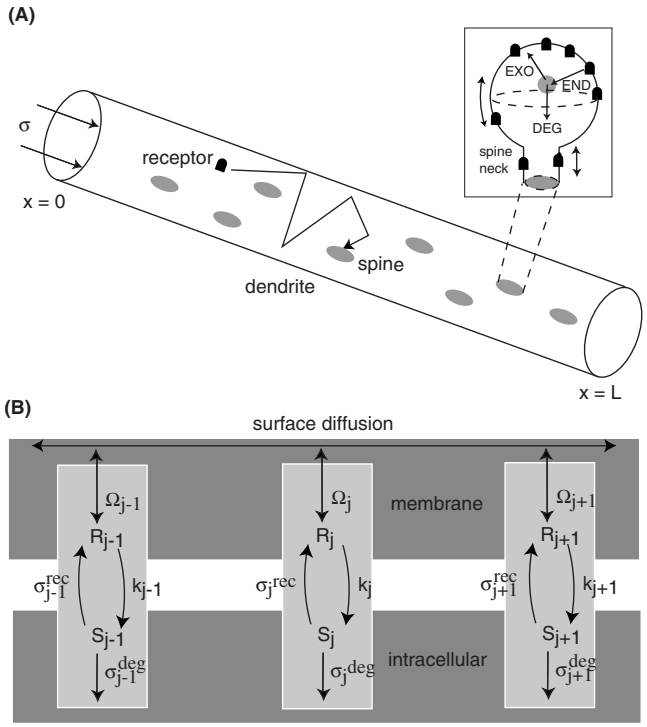

FIG. 1. Diffusion-trapping model of receptor trafficking along a dendritic cable (diagrams not to scale). (A) A population of dendritic spines are distributed on the surface of a dendritic cable of length L. Each receptor diffuses freely until it encounters a spine where it may become trapped. Within a spine receptors may be internalized via endocytosis (END) and then either recycled to the surface via exocytosis (EXO) or degraded (DEG), see inset. Synthesis of new receptors at the soma and insertion into the plasma membrane generates a surface flux σ at one end of the cable. (B) Reduced one-dimensional model showing a set of discrete trapping sites (spines) and their associated state transition diagrams. Here R_j denotes the concentration of surface receptors inside the jth spine, and S_j denotes the number of receptors within the corresponding intracellular pool. Freely diffusing surface receptors can enter/exit the spine at a hopping rate Ω_j, be endocytosed at a rate k_j, exocytosed at a rate σ_j^{rec}, and degraded at a rate σ_j^{deg}. The spatial extent of each trapping region is neglected so that free diffusion occurs over the whole length of the cable.

efficacy of diffusive transport depends on various biophysical parameters such as the surface diffusivity and the rates of exo- and endocytosis within a spine.

It should be noted that diffusion-trapping problems arise in many areas of physics, chemistry, and biology, and a variety of different modeling techniques have been developed to study them. For example, in random porous media a particle diffuses freely in a pore region until it encounters the boundary of a partially absorbing trap region (pore-trap interface) where it is absorbed with some probability. Here the spatial extent of the trap regions are not negligible so that one has to solve the diffusion equation in a heterogeneous medium using techniques such as homogenization theory [15,16]. Another important class of model is that of continuous time random walks [17,18], which have been used to study anomalous transport in a wide range of systems including motor proteins [19]. In these spatially discrete models the effect of a trap is to generate a nonexponential waiting time distribution. In terms of a spatially discrete version of our receptor trafficking model, only a fraction of sites (corresponding to spines) would have waiting time distributions that differ from a simple exponential—these sites do not generate anomalous diffusion but modify the diffusivity of the system on large time scales.

II. DIFFUSION-TRAPPING MODEL

Consider a population of N spines distributed along a uniform dendritic cable of length L, with x_j, $j=1,\ldots,N$, the position (axial coordinate) of the jth spine. Let $U(x,t)$ denote the concentration (per unit length) of surface receptors within the dendritic membrane at position x at time t and let $R_j(t)$ denote the concentration (per unit area) of surface receptors trapped at the jth spine. The dendritic surface receptor concentration evolves according to the diffusion equation

$$\frac{\partial U}{\partial t} = D\frac{\partial^2 U}{\partial x^2} - \sum_{j=1}^{N} \Omega_j [U_j - R_j]\delta(x - x_j), \tag{1}$$

where D is the surface diffusivity, $U_j(t)=U(x_j,t)/l$, and l is the circumference of the cable (with $l \ll L$). The first term on the right-hand side of Eq. (1) represents the Brownian diffusion of receptors along the surface of the cable. The second term on the right-hand side represents the total number of receptors per unit time that flow into or out of the spines. The contribution from the jth spine is taken to depend on the difference in concentrations (per unit area) across the junction between the spine and dendritic cable with Ω_j an effective hopping rate. (This rate depends on the detailed geometry of the dendritic spine [20].) Equation (1) is supplemented by the following boundary conditions at the ends of the cable $x=0,L$:

$$D\left.\frac{\partial U}{\partial x}\right|_{x=0} = -\sigma, \quad D\left.\frac{\partial U}{\partial x}\right|_{x=L} = 0. \tag{2}$$

Here σ is the number of receptors per unit time entering the cable from the soma at $x=0$. The distal end of the cable is assumed to be closed.

Surface receptors within the jth spine can be endocytosed at a rate k_j and stored in an intracellular pool. Intracellular receptors are either reinserted into the surface via exocytosis at a rate σ_j^{rec} or degraded at a rate σ_j^{deg}. Denoting the number of receptors in the jth intracellular pool by $S_j(t)$, we have the pair of equations

$$\frac{dR_j}{dt} = \frac{\Omega_j}{A_j}[U_j - R_j] - k_j R_j + \frac{\sigma_j^{rec} S_j}{A_j}, \tag{3}$$

$$\frac{dS_j}{dt} = -\sigma_j^{rec} S_j - \sigma_j^{deg} S_j + A_j k_j R_j. \tag{4}$$

The first term on the right-hand side of Eq. (3) represents the exchange of surface receptors between the spine and parent dendrite. Since $\Omega_j[U_j - R_j]$ is the number of receptors per unit time flowing across the junction between the dendritic

cable and the spine, it is necessary to divide through by the surface area A_j of the spine in order to properly conserve receptor numbers. The various processes described by Eqs. (3) and (4) are summarized in Fig. 1(B).

III. STEADY-STATE SOLUTION

Equations (3) and (4) show that in steady state,

$$R_j = \frac{\Omega_j U_j}{\Omega_j + A_j k_j (1-\lambda_j)}, \quad S_j = \frac{A_j k_j R_j}{\sigma_j^{rec} + \sigma_j^{deg}} \tag{5}$$

with

$$\lambda_j = \frac{\sigma_j^{rec}}{\sigma_j^{rec} + \sigma_j^{deg}} \tag{6}$$

and U_j determined from the steady-state version of Eq. (1):

$$0 = D\frac{d^2U}{dx^2} - \sum_{j=1}^{N} b_j U_j \delta(x - x_j), \tag{7}$$

where

$$b_j = \frac{\Omega_j A_j k_j (1-\lambda_j)}{\Omega_j + A_j k_j (1-\lambda_j)}. \tag{8}$$

Integrating Eq. (7) over the interval $0 \leqslant x \leqslant L$ leads to the self-consistency condition

$$\sigma = \sum_{j=1}^{N} b_j U_j. \tag{9}$$

This ensures the conservation of receptors entering and leaving the dendrite. Equation (7) can be solved in terms of the generalized one-dimensional Green's function $G(x,x')$, which satisfies the equation

$$\frac{d^2G(x,x')}{dx^2} = -\delta(x-x') + L^{-1}, \tag{10}$$

with reflecting boundary conditions at the ends $x=0,L$. A standard calculation shows that

$$G(x,x') = \frac{L}{12}\{h([x+x']/L) + h(|x-x'|/L)\}, \tag{11}$$

where $h(x)=3x^2-6|x|+2$. Given the Green's function G, the dendritic surface receptor concentration has an implicit solution of the form

$$U(x) = \chi - \sum_{j=1}^{N} \frac{b_j U_j}{D} G(x,x_j) + \frac{\sigma}{D} G(x,0), \tag{12}$$

where the constant χ is determined from the self-consistency condition (9).

We can now generate a matrix equation for the concentration of dendritic receptors U_i at the ith spine, $i=1,\ldots,N$, by setting $x=x_i$ in Eq. (12) and dividing through by the circumference l:

$$U_i = \frac{\chi}{l} - \sum_{j=1}^{N} \mathcal{G}_{ij} U_j + \sigma g_i, \tag{13}$$

where

$$\mathcal{G}_{ij} = \frac{b_j}{lD} G(x_i,x_j), \quad g_i = \frac{1}{lD} G(x_i,0). \tag{14}$$

If the matrix $\mathcal{G}=(\mathcal{G}_{ij})$ does not have -1 as an eigenvalue (which is the generic case), then the matrix $\mathcal{I}+\mathcal{G}$, where $\mathcal{I}$ is the $N\times N$ identity matrix, is invertible and we can solve the system (13). That is, setting $\mathcal{M}=(\mathcal{I}+\mathcal{G})^{-1}$, we have

$$U_i = \sum_j \mathcal{M}_{ij}[\chi/l + \sigma g_j]. \tag{15}$$

The self-consistency condition (9) then determines χ according to

$$\frac{\chi}{l} = \sigma \left[\frac{1 - \sum_{k,l} b_k \mathcal{M}_{kl} g_l}{\sum_{k,l} b_k \mathcal{M}_{kl}} \right]. \tag{16}$$

Equations (15) and (16) determine the dendritic receptor concentration U_j at the discrete site x_j of the jth dendritic spine. Substituting this solution into Eq. (12) then generates the full receptor concentration profile $U(x)$. Similarly, substituting Eqs. (15) and (16) into Eq. (5) determines the number of receptors at the surface of each spine, A_jR_j, and the number of receptors in each intracellular pool, S_j. We note that U_j and, hence, $U(x)$, R_j, S_j all scale multiplicatively with the somatic flux σ.

A. Uniform spines

The matrix solution for U_i given by Eqs. (15) and (16) is very useful for numerically determining the distribution of receptors in the general heterogeneous case. However, in the case of identical spines distributed uniformly along the cable, we can use a continuum approximation to derive a more analytically convenient expression for $U(x)$. Therefore consider a set of N identical spines with uniform spacing $d=L/N$ such that $x_j=jd$, $j=1,\ldots,N$. We then rewrite Eq. (7) in the form

$$0 = D\frac{d^2U}{dx^2} - \frac{b}{l}\rho U, \tag{17}$$

where $\rho=\Sigma_{j=1}^{N}\delta(x-jd)$ and $b_j=b$ for all $j=1,\ldots,N$. In the case of large N, we can approximate ρ by the uniform distribution $\rho=N/L=1/d$ and then solve the resulting differential equation. Imposing the boundary conditions (2) yields the solution

$$U(x) = \frac{\sigma}{D\Lambda_0} \frac{\cosh(\Lambda_0[L-x])}{\sinh(\Lambda_0 L)}, \tag{18}$$

where

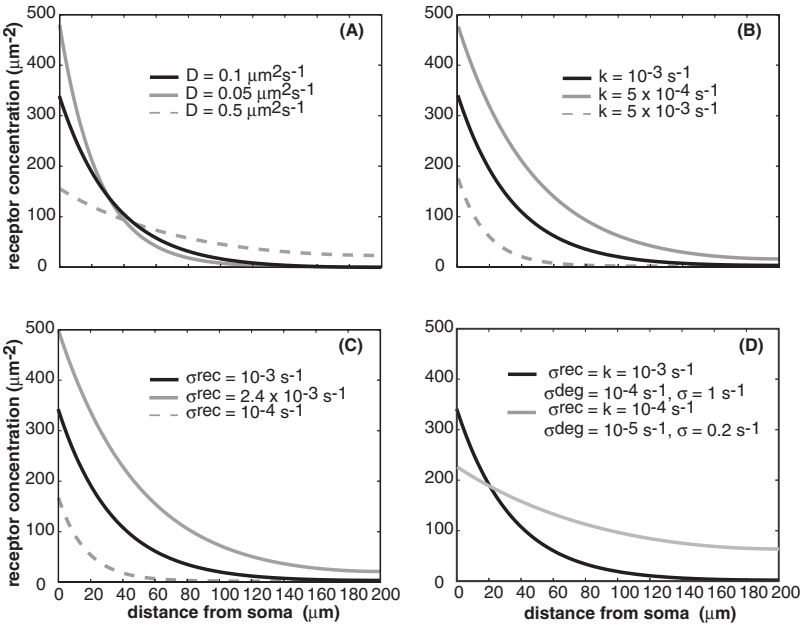

FIG. 2. Dendritic receptor concentration plotted as a function of distance from the soma for a uniform distribution of identical spines. The dendritic cable has length $L=200$ μm and circumference $l=1$ μm. We consider $N=200$ spines having spacing $d=1$ μm and surface area $A=1$ μm^2. (A)–(D) The black curve is the receptor profile for the following baseline parameter values: $D=0.1$ μm^2 s^{-1}, $k=10^{-3}$ s^{-1}, $\Omega=10^{-3}$ μm^2 s^{-1}, $\sigma^{rec}=10^{-3}$ s^{-1} and $\sigma^{deg}=10^{-4}$ s^{-1} (so that $\lambda=0.909$), and $\sigma=1$ s^{-1}. Gray curves correspond to receptor profiles when one or more parameters are changed from the baseline as indicated.

$$\Lambda_0 = \sqrt{\frac{b}{ldD}}, \quad b = \frac{\Omega A k(1-\lambda)}{\Omega + Ak(1-\lambda)}, \tag{19}$$

i.e., b is given by the j-independent version of Eq. (8). The continuum approximation thus implies that the dendritic receptor concentration $U(x)$ is an exponentially decaying function of the distance x from the soma with an effective space constant Λ_0. It follows that for a given L, an approximately flat distribution can be obtained provided that $\Lambda_0 L \ll 1$; the magnitude of the receptor concentration will then depend on the somatic flux σ.

In Fig. 2 we plot the steady-state receptor concentration in the dendritic membrane as a function of distance from the soma, based on Eqs. (12), (15), and (16). We consider $N=200$ identical spines of surface area $A=1$ μm^2 distributed uniformly along a cable of length $L=200$ μm and circumference $l=1$ μm. In Figs. 2(A)–2(D) the black curve shows the receptor profile for the following baseline parameter values, which are consistent with typical values reported experimentally: diffusivity $D=0.1$ μm^2 s^{-1} [9,20], rate of endocytosis $k=10^{-3}$ s^{-1} [10,21], hopping rate $\Omega=10^{-3}$ μm^2 s^{-1} [13,20], and rate of exocytosis $\sigma^{rec}=10^{-3}$ s^{-1} [10]. (However, see Ref. [4] which suggests that the local rates of exocytosis/endocytosis could be at least an order of magnitude slower.) We choose a rate of degradation $\sigma^{deg}=10^{-4}$ s^{-1} (so that $\lambda=0.909$) and a somatic flux $\sigma=1$ s^{-1} (so that the receptor concentrations close to the soma are physiologically reasonable). The gray curves then show how the profile changes when one or more parameters are changed from baseline. In Figs. 2(A)–2(C) we plot receptor profiles for different values of the diffusivity D, endocytic rate k, and recycling rate σ^{rec}. As expected, larger (smaller) values of D lead to more (less) diffuse receptor profiles. Increasing k causes there to be less receptors on the dendritic membrane (and in spines), but more in intracellular pools, while decreasing k has the opposite effect. Increasing σ^{rec}, and hence λ, forces more receptors into the dendritic membrane (and spines) at the expense of the number of receptors in intracellular pools, while decreasing σ^{rec} has the opposite effect. These results can also be understood from the continuum approximation, which shows that the correlation length Λ_0^{-1} and maximum concentration $U(0)$ increase as σ^{rec} increases or k decreases. On the other hand, Λ_0^{-1} increases with D whereas $U(0)$ decreases with D. In Fig. 2(D) we show an example of an approximately flat receptor distribution (over the given cable length L), obtained by taking rates of exo/endocytosis more consistent with Ref. [4] and by reducing the somatic flux σ and rate of degradation σ^{deg} accordingly.

The above analysis provides a quantitative measure of the rate of decay of the dendritic receptor concentration $U(x)$ with distance from the soma and its dependence on various biophysical parameters. The corresponding number of receptors in each spine can then be determined from Eq. (5). For the physiologically based parameter values used in Fig. 2 we find that numerically $R_j \approx U_j$. Our results thus suggest that it is not possible to maintain receptor numbers in spines located beyond a few hundred μm unless the rate of degradation is sufficiently slow, as suggested by Ref. [4]. However, on longer length scales one confronts another well-known limitation regarding diffusion-based transport, namely, that the characteristic time τ to travel a distance X varies as $\tau=X^2/2D$. Taking typical measured values of the diffusivity ($D=0.1$ μm^2 s^{-1}) [9,20], the time to travel 100 μm from the soma is then $T=5\times10^4$ s$\approx$15 h. Given that the lifetime of an AMPA receptor is approximately one day [22], this suggests that receptors will not be able to diffuse beyond around 150 μm (unless constitutive recycling provides a way to extend the effective lifetime of a receptor). We show in Sec. IV that taking $\tau=X^2/2D$ is an underestimate of the characteristic time τ, since it does not take into account the effects of trapping by spines.

B. Nonuniform spines

There is a considerable amount of heterogeneity in the properties and spatial distribution of spines in a single neu-

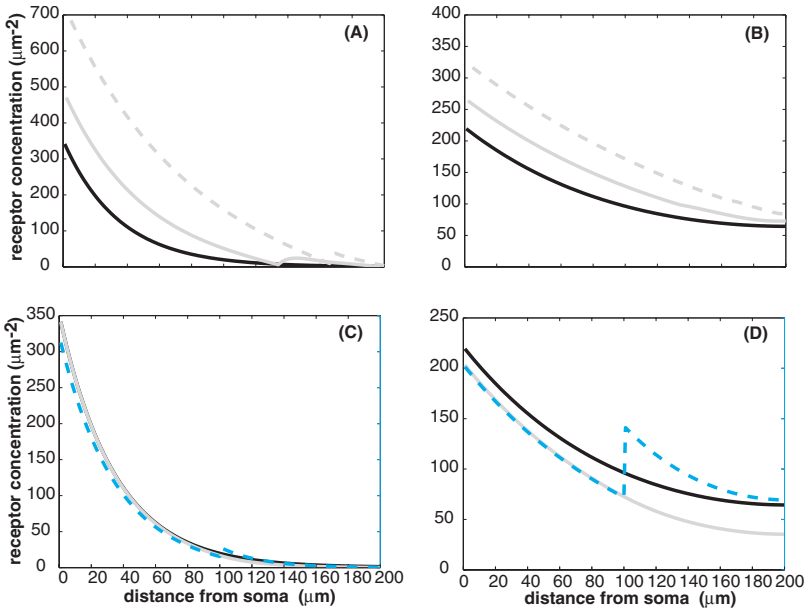

FIG. 3. (Color online) Inhomogeneities in spine density and surface area. (A) Dendritic receptor concentration plotted as a function of distance from the soma for various distributions of identical spines: spines are spaced 2 μm apart for the first 134 μm of the cable, then 0.5 μm thereafter (solid gray line), or spaced 4.88 μm for the first 166 μm of the cable, then 0.205 μm thereafter (dashed gray line); all other parameters are taken at baseline as defined in Fig. 2. Note that for both distributions the total number of spines is still $N=200$. In both cases there are more receptors at each location of the cable than in the uniform distribution (black). (B) Same as (A), except parameters are chosen as in Fig. 2(D). Again, there are more receptors everywhere. (C) Dendritic receptor concentration (solid gray line) and receptor numbers in spines (dashed blue line) plotted as functions of distance from the soma for a uniform distribution of nonidentical spines. (The numerical range of both quantities are taken to be the same.) Spine surface area is 1 μm^2 for the first 100 μm of the cable, then 2 μm^2 thereafter; all other parameters are taken at baseline as defined in Fig. 2. There is relatively little change from baseline (black). (D) Same as (C), except parameters are chosen as in Fig. 2(D). Receptor numbers at spines increase dramatically beginning 100 μm from the soma.

ron (reviewed in Ref. [23]). For example, spine densities typically increase with distance from the soma, peak at some distance between the soma and the distal end of the dendrite, then decrease thereafter [24]. Spine morphology ranges from small filopodial protrusions to large mushroomlike bulbs, and properties such as the surface area A also vary systematically along the dendrite [25]. These heterogeneities can be taken into account using our general solution for the steady-state receptor concentration, Eqs. (12), (15), and (16). We illustrate this in Fig. 3, where we present plots similar to those in Fig. 2 except that now we allow the density and surface area of spines to vary. In Figs. 3(A) and 3(B) the dendritic receptor concentration is plotted for two inhomogeneous distributions of identical spines: one in which spines are spaced 2 μm apart for the first 134 μm of the cable, then 0.5 μm thereafter, and another wherein spines are spaced 4.88 μm for the first 166 μm of the cable, then 0.205 μm thereafter. These spacings were chosen so that the total number of spines remains $N=200$. In both cases there are more receptors at each location along the length of the dendritic cable than there are for a uniform distribution of spines, due to the fact that there are less spines near the soma, allowing receptor concentrations to build up along the length of the cable. In Figs. 3(C) and 3(D) we plot the dendritic receptor concentration and receptor spine numbers as functions of distance from the soma for a uniform distribution of nonidentical spines: spine surface area is taken to be 1 μm^2 for the first 100 μm of the cable, then 2 μm^2 thereafter. There is relatively little change from baseline when parameter values are taken as in Fig. 2(A). However, when parameter values are taken as in Fig. 2(D), receptor numbers at spines increase markedly from baseline beginning 100 μm from the soma, although dendritic receptor concentrations are everywhere less than baseline.

IV. MEAN FIRST PASSAGE TIME (MFPT)

In this section we calculate the MFPT for a single tagged particle to travel a distance X from the soma and use this to determine an effective diffusivity, which takes into account the effects of trapping at spines. Since we are assuming that the tagged particle has not been degraded over the time interval of interest we set $\sigma_j^{deg}=0$ for all j. Let $\tau(X)$ denote the time it takes for a particle starting at the soma to first reach a distance X along the cable. Since the movement of a single receptor within the surface of the dendritic cable is driven by diffusion, τ is a random variable and we are therefore interested in calculating the mean of τ, which we denote by T. Hence we wish to solve a MFPT problem for the Fokker-Planck equations

$$\frac{\partial u}{\partial t} = D\frac{\partial^2 u}{\partial x^2} - \sum_{j=1}^{N} \Omega_j [u_j - r_j/A_j]\delta(x - x_j), \tag{20}$$

$$\frac{dr_j}{dt} = \Omega_j [u_j - r_j/A_j] - k_j r_j + \sigma_j^{rec} s_j, \tag{21}$$

$$\frac{ds_j}{dt} = -\sigma_j^{rec} s_j + k_j r_j. \tag{22}$$

Here the lower case variable $u(x,t)$ represents the probability density (per unit length) that at time $t \geqslant 0$ the receptor is not trapped at a spine and is located at a distance x along the cable. Similarly, $r_j(t)$ and $s_j(t)$ represent the probabilities, respectively, that at time $t \geqslant 0$ the receptor is either at the surface of the jth spine or is in the corresponding intracellular pool. The initial conditions are $u(x,0)=\delta(x)$ and $r_j(0)=s_j(0)=0$ for all j.

We calculate the MFPT by solving Eq. (20) on the interval $[0,X)$ supplemented by a reflecting boundary condition at $x=0$ and an absorbing boundary condition at $x=X$. The absorbing boundary condition removes the receptor once it reaches a distance X from the soma and represents the fact that we are only interested in the time it takes for a receptor to first reach this distance given that it started at the origin. The function

$$F(X,t) \equiv \int_0^X u(x,t)dx + \sum_{j=1}^{N_X} [r_j(t) + s_j(t)] \tag{23}$$

is the probability that $t < \tau(X)$; i.e., the probability that a receptor which was initially at the origin has not yet reached the point $x=X$ in a time t. Here N_X is the number of spines in the interval $[0,X)$. Notice that $1-F$ is the cumulative density function for τ, hence

$$\frac{\partial(1-F)}{\partial t} = -\frac{\partial F}{\partial t} \tag{24}$$

is its probability density function. Thus the MFPT T is

$$T = -\int_0^\infty t\frac{\partial F}{\partial t}dt = \int_0^\infty F dt. \tag{25}$$

The last equality in Eq. (25) follows by integrating the first integral by parts and recalling that F, being an L^1 function in time, decays more rapidly to zero than t^{-1} as t becomes large. Therefore integrating Eq. (23) over time gives us the following expression for $T(x)$:

$$T(X) = \int_0^X \hat{u}(x,0)dx + \sum_{j=1}^{N_X} [\hat{r}_j(0) + \hat{s}_j(0)], \tag{26}$$

where $\hat{\cdot}$ denotes the Laplace transform with respect to time,

$$\hat{f}(z) \equiv \int_0^\infty e^{-zt} f(t)dt. \tag{27}$$

Laplace transforming Eqs. (20)–(22) and using the initial conditions, we find

$$-z\hat{u} + D\frac{\partial^2 \hat{u}}{\partial x^2} = \sum_{j=1}^{N_X} \Omega_j[\hat{u}_j - \hat{r}_j/A_j]\delta(x-x_j) - \delta(x), \tag{28}$$

$$z\hat{r}_j = \Omega_j[\hat{u}_j - \hat{r}_j/A_j] - k_j\hat{r}_j + \sigma_j^{rec}\hat{s}_j, \tag{29}$$

$$z\hat{s}_j = -\sigma_j^{rec}\hat{s}_j + k_j\hat{r}_j, \tag{30}$$

where $\hat{u}_j(z)=\hat{u}(x_j,z)/l$. In the limit $z \to 0$, Eqs. (29) and (30) show that

$$A_j\hat{u}_j(0) = \hat{r}_j(0) = \frac{\sigma_j^{rec}}{k_j}\hat{s}_j(0) \tag{31}$$

and Eq. (28) becomes

$$D\frac{\partial^2 \hat{u}(x,0)}{\partial x^2} = -\delta(x). \tag{32}$$

Imposing the boundary conditions at $x=0,X$ leads to the solution

$$\hat{u}(x,0) = \frac{X-x}{D}. \tag{33}$$

From Eqs. (26), (31), and (33) we then calculate $T(X)$:

$$T(X) = \frac{X^2}{2D} + \frac{1}{D}\sum_{j=1}^{N_X} \eta_j(X-x_j), \tag{34}$$

where $\eta_j = A_j[1+k_j/\sigma_j^{rec}]/l$. The first term on the right-hand side of this equation is the MFPT in the absence of any spines, whereas the remaining terms take into account the effects of being temporarily trapped at a spine.

In order to calculate an effective diffusivity, let us consider the simple example of identical spines distributed uniformly along the cable with spacing d. That is, we take the site of the jth spine to be $x_j=jd$, $j=1,\ldots,N$ such that $Nd=L$. We also set $N_X=X/d$. Equation (34) then becomes (for $N_X \gg 1$)

$$T(X) = \frac{X^2}{2D} + \frac{\eta}{D}\sum_{j=1}^{N_X}(X-jd) = \frac{X^2}{2D} + \frac{\eta}{D}\left(N_X X - \frac{(N_X+1)N_X d}{2}\right)$$

$$\approx \frac{X^2}{2D} + \frac{\eta}{D}\frac{X^2}{2d} = \frac{X^2}{2D_{eff}},$$

where

$$D_{eff} = \frac{D}{1 + \frac{A}{ld}\left(1 + \frac{k}{\sigma^{rec}}\right)}. \tag{35}$$

As one would expect, the presence of traps reduces the effective diffusivity of a receptor. In particular, the diffusivity is reduced by increasing the ratio k/σ^{rec} of the rates of endocytosis and exocytosis or by increasing the surface area A of a spine relative to the product of the spine spacing d and circumference of the cable l. Interestingly, D_{eff} does not depend on the hopping rate Ω. At first sight this might seem counterintuitive, since a smaller Ω implies that a receptor finds it more difficult to exit a spine so the effective residence time within the spine increases. However, this is compensated by the fact that it is also more difficult for a receptor to enter a spine in the first place. (For a more detailed analysis of entry/exit times of receptors with respect to spines see Ref. [26].)

For the sake of illustration, suppose that the rates of exo/endocytosis are equal ($k=\sigma^{rec}$). Taking typical measured values of the diffusivity ($D=0.1\ \mu m^2\ s^{-1}$) [9,20], the area of a spine ($A=1\ \mu m^2$), the spacing between spines ($d=1\ \mu m$), and the circumference of a dendrite ($l=1\ \mu m$) [12], we find $D_{eff}=0.5D$. The corresponding MFTP to travel 100 μm from the soma is then $T=10^5$ s ≈ 30 h. The distance that a receptor can diffuse would be further reduced if $k \gg \sigma^{rec}$ such that $D_{eff} \ll D$. As we have previously indicated, there is currently some controversy regarding the absolute rates of exo/endocytosis for AMPA receptors [4,21], although there is growing evidence that their values are activity dependent [10] so that the ratio k/σ^{rec} and, hence D_{eff}, may be modifiable by experience.

V. DISCUSSION

In this paper we presented a diffusion-trapping model for the surface transport of receptors along a dendritic cable. Within each spatially localized trapping region (dendritic spine) a receptor could be internalized via endocytosis and then either recycled to the surface via exocytosis or degraded. The effects of the spines were twofold. First, they reduced the effective surface diffusivity of receptors. Second, they resulted in a spatially decaying profile for the steady-state receptor concentration along the cable, assuming that new receptors are synthesized at the soma and then inserted into the plasma membrane at the proximal end of the dendrite. Using physiologically reasonable parameter values we found that it was not possible for surface diffusion to supply spines with receptors beyond a few hundred μm from the soma. This suggests that an additional mechanism is needed in order to transport receptors to more distal spines. One possibility is that newly synthesized receptors are stored locally within intracellular pools: these receptors are either synthesized locally or they are synthesized at the soma and then transported intracellularly along microtubules from the soma to local pools [1,8]. Our model could be modified accordingly by introducing a source term into the kinetic equation for the number of intracellular receptors, see Eq. (4). Newly synthesized receptors would then be transported from the intracellular pool to the surface membrane via exocytosis, being inserted directly into a synapse or into neighboring regions of the spine and dendrite [21]; in the latter case local surface diffusion would provide the final step in delivering receptors to the synapse.

Although we have established that surface diffusion cannot be the sole mechanism for delivering receptors from the soma to synapses, it still plays an important role in receptor trafficking. In particular, the concentration of receptors within a spine depends on the local dendritic receptor concentration which, in turn, depends on the distribution of receptors across all spines; this nonlocal interaction is mediated by surface diffusion [see Eqs. (1) and (3)]. There is a growing body of experimental evidence suggesting that the trafficking of AMPA receptors into and out of spines contributes to activity-dependent, long-lasting changes in synaptic strength [27,28]. Therefore understanding the nonlocal effects of surface receptor diffusion along a dendrite could have important implications for synaptic plasticity. We hope to explore this issue further elsewhere.

ACKNOWLEDGMENTS

This work was supported by the National Science Foundation (Grant Nos. DMS 0515725 and RTG 0354259).

[1] M. J. Kennedy and M. D. Ehlers, Annu. Rev. Neurosci. **29**, 325 (2006).
[2] D. Choquet and A. Triller, Nat. Rev. Neurosci. **4**, 251 (2003).
[3] A. Triller and D. Choquet, Trends Neurosci. **28**, 133 (2005).
[4] H. Adesnik, R. A. Nicoll, and P. M. England, Neuron **48**, 977 (2005).
[5] C.-H. Kim and J. E. Lisman, J. Neurosci. **21**, 4188 (2001).
[6] M. Setou, D. H. Seog, Y. Tanaka, Y. Kanai, Y. Takei, and N. Hirokawa, Nature (London) **417**, 83 (2002).
[7] P. Washbourne, X.-B. Liu, E. G. Jones, and A. K. McAllister, J. Neurosci. **24**, 8253 (2004).
[8] P. C. Bressloff, Phys. Rev. E **74**, 031910 (2006).
[9] L. Groc, M. Heine, L. Cognet, K. Brickley, F. A. Stephenson, B. Lounis, and D. Choquet, Nat. Neurosci. **7**, 695 (2004).
[10] M. D. Ehlers, Neuron **28**, 511 (2000).
[11] L. Chen, T. Tracy, and C. I. Nam, Curr. Opin. Neurobiol. **17**, 53 (2007).
[12] K. E. Sorra and K. M. Harris, Hippocampus **10**, 501 (2000).
[13] B. A. Earnshaw and P. C. Bressloff, J. Neurosci. **26**, 12362 (2006).
[14] D. Holcman and A. Triller, Biophys. J. **91**, 2405 (2006).
[15] J. Rubinstein and S. Torquato, J. Chem. Phys. **88**, 6372 (1988).
[16] S. Torquato, *Random Heterogeneous Materials* (Springer-Verlag, New York, 2002).
[17] H. Scher and E. W. Montroll, Phys. Rev. B **12**, 2455 (1975).
[18] B. D. Hughes, *Random Walks and Random Environments* (Clarendon Press, Oxford, 1995).
[19] A. B. Kolomeisky and M. E. Fisher, J. Chem. Phys. **113**, 10867 (2000).
[20] M. C. Ashby, S. R. Maier, A. Nishimune, and J. M. Henley, J. Neurosci. **26**, 7046 (2006).
[21] M. Passafaro, V. Piech, and M. Sheng, Nat. Neurosci. **4**, 917 (2001).
[22] K. Archibald, M. J. Perry, E. Molnar, and J. M. Henley, Int. J. Neuropharmacol. **37**, 1345 (1998).
[23] E. A. Nimchinsky, B. L. Sabatini, and K. Svoboda, Annu. Rev. Physiol. **64**, 313 (2002).
[24] M. Marin-Padilla, J. Comp. Neurol. **131**, 475 (1967).
[25] S. Konur, D. Rabinowitz, V. L. Fenstermaker, and R. Yuste, J. Neurobiol. **56**, 95 (2003).
[26] D. Holcman and Z. Schuss, J. Stat. Phys. **117**, 975 (2004).
[27] D. S. Bredt and R. A. Nicoll, Neuron **40**, 361 (2003).
[28] V. A. Derkach, M. C. Oh, E. S. Guire, and T. S. Soderling, Nat. Rev. Neurosci. **8**, 101 (2007).